

## Simultaneous Kinetic-Potentiometric Determination of Aluminum(III) and Iron(II)

M.A. KARIMI\*<sup>†</sup>, M. MAZLOUM ARDAKANI<sup>‡</sup> and N. ZAREA ZADEH<sup>†</sup>

*Department of Chemistry, Faculty of Sciences, Payame Noor University (PNU), Sirjan, Iran*

*Fax: (98)(345)5233540; E-mail: m\_karimi@pnu.ac.ir; ma\_karimi43@yahoo.com*

The H-point standard addition method (HPSAM), partial least squares (PLS) and principal component regression (PCR) are suggested in this study for simple and accurate simultaneous determination of Fe(II) and Al(III). In this work, the oxidation reaction of Fe(II) to Fe(III) in the presence of peracetic acid (PAA) as oxidant is based of the method. The complexing reaction of Fe(III) and Al(III) with fluoride ion has a difference rate at certain reaction conditions. So the exist of oxidant is necessary for oxidation of Fe(II) to Fe(III) that has no effect on Al(III) ion. The rate of consume fluoride ion for making complex is detected with a fluoride ion selective electrode (FISE). The results show that simultaneous determination of Fe(II) and Al(III) can be done in their concentration ranges of 0.5-40.0 and 1.0-25.0  $\mu\text{g mL}^{-1}$ , respectively. The total relative standard error for applying the PLS and PCR methods on 8 synthetic samples was 3.43 and 3.85, respectively in the concentration ranges of 3.0-25.0  $\mu\text{g mL}^{-1}$  of Fe(II) and 3.0-15.0  $\mu\text{g mL}^{-1}$  of Al(III). The proposed methods (HPSAM, PLS and PCR) were applied to the simultaneous determination of Fe(II) and Al(III) in different water samples.

**Key Words:** Simultaneous determination, Kinetic-potentiometric, Iron(II), Aluminium(III), Fluoride ion selective electrode, H-point standard addition method, Partial least squares, Principal component regression (PCR).

### INTRODUCTION

Aluminum and iron are metal ions which appear together in a wide variety of environmental, industrial and geometrical samples. There are many analytical techniques for the determination of Al and Fe including spectrophotometry<sup>1</sup>, inductively coupled plasma-atomic emission spectrometry (ICP-AES)<sup>2</sup>, atomic emission spectroscopy (AAS)<sup>3</sup> and electroanalytical methods<sup>4</sup>. Several methods have been reported for the determination of Al and Fe simultaneously using chemometrics methods. Chemometrics methods such as partial least squares (PLS), principal component regression (PCR) and artificial neural network (ANN) was reported for simultaneous

<sup>†</sup>Department of Chemistry, Faculty of Sciences, Payame Noor University (PNU), Ardakan, Iran.

<sup>‡</sup>Department of Chemistry, Faculty of Sciences, Yazd University, Yazd 89195-741, I.R. Iran.

spectrophotometric determination of binary mixtures of Al(III) and Fe(III) and also for Al(III) and Fe(II) mixtures in different samples<sup>5-8</sup>. To the best of our knowledge, there is not any report for using of H-point standard addition method (HPSAM) and chemometrics methods for simultaneous determination of Fe(II) and Al(III) based on kinetic-potentiometric data or other electroanalytical methods.

In recent years the usage of chemometrics methods in electroanalytical chemistry, as in other areas of analytical chemistry, has received considerable attention as these methods can help us with extraction of more information from experimental data. Applications of HPSAM and chemometrics methods have been frequently reported for the calibration of overlapped voltammetric signals<sup>8-13</sup>. In the field of potentiometry, several methods have been reported based on flow injection system and titration using PLS, ANN and Kalman filter as modeling methods<sup>14-20</sup>. Recently, we reported the first application of PLS and PCR multivariate calibration methods and HPSAM to the simultaneous kinetic-potentiometric determination of binary mixtures of hydrazine and its derivatives and also binary mixture of levodopa and carbidopa drugs<sup>21-23</sup>. The methods were based on the differences observed in the production rate of chloride ions in reaction of these species with N-chlorosuccinimide. The reaction rate of production of chloride ion was monitored by a chloride ion-selective electrode.

This paper reports the first application of HPSAM, PCR and PLS to the simultaneous determination of Fe(II) and Al(III) of metallic ions using potentiometric technique and ion-selective electrodes (ISEs). The method is based on the oxidation reaction of Fe(II) to Fe(III) in the presence of peracetic acid (PAA) as oxidant and complexing reaction between Fe(III) and Al(III) with fluoride ion which has a differential rate at certain reaction conditions. The fast response of the FISE and its Nernstian behaviour with respect to fluoride ions in acidic solutions indicated that this electrode might be employed effectively in kinetic studies of reactions involving changes in the fluoride ion concentration<sup>19</sup>. Therefore, rate of the complexing reaction of fluoride ion with Fe(III) and Al(III) was monitored by a FISE.

## EXPERIMENTAL

A solid-state fluoride-selective electrode (Metrohm Model 6.0502.150) was used in conjunction with a double junction Ag/AgCl reference electrode (Metrohm Model 6.0726.100), whose outer compartment was filled with a saturated KCl solution. The Metrohm Model 780 potentiometer, attached to a Pentium(IV) computer, was used for recording the kinetic potentiometric data. All measurements were carried out in a thermostated ( $25.0 \pm 0.2$  °C), double-walled reaction cell with continuous magnetic stirring. The electrode was stored in  $1 \times 10^{-3}$  M potassium fluoride solution when not in use. For pH measurements, a Metrohm Model 780 pH meter with combination glass electrode was used. Chemometrics analysis was performed using MATLAB 7.0 program.

All chemicals were of analytical reagent grade and doubly distilled water was used throughout. A stock solution of iron ( $1000 \mu\text{g mL}^{-1}$ ) was prepared by dissolving 0.524 g of iron(II) sulfate ( $\text{FeSO}_4 \cdot 7\text{H}_2\text{O}$ ) in water and diluted to 100 mL. A stock solution of aluminum ( $1000 \mu\text{g mL}^{-1}$ ) was prepared by dissolving 0.4943 g of aluminum chloride in water and diluted to 100 mL. A standard fluoride solution (0.1 M) was prepared by dissolving 0.4199 g of sodium fluoride in distilled water and diluting to 100 mL. A standard peracetic acid (PAA) solution (0.05 M) was prepared by peracetic acid (39.4 %) to the desired volume with water. This solution was made daily and kept at  $4^\circ\text{C}$  in an amber-coloured bottle in dark. The iron(II) stock solution was also protected from exposure to air and light. The peracetic acid and salts of Al(III) or Fe(III) and fluoride were purchased from Merck (Germany). Acetate buffer solution (0.05 M, pH 3.0) was prepared using acetic acid and NaOH solutions and adjusting its pH with a pH meter.

**Procedure:** Twenty five milliliters of double distilled water, 2.0 mL of buffer solution, 1.0 mL of standard fluoride solution ( $0.1 \text{ mol L}^{-1}$ ) and 1.0 mL of standard PAA solution were added to the thermostated ( $25.0 \pm 0.2^\circ\text{C}$ ) reaction cell. Five milliliter of the standard or sample solution of Al(III) or Fe(II) or a mixture of them were injected into the cell quickly and after the stabilization of the potential (about 20 s), all data were recorded. The potential changes *versus* time were recorded at the time intervals of 1.0 s. Synthetic samples containing different concentration ratios of Al(III) and Fe(II) were prepared and standard additions of Al(III) were made. Simultaneous determination of Al(III) and Fe(II) was conducted by recording the potential changes for each solution from 20 to 130 s. After each run the cell was emptied and washed twice with doubly distilled water.

Using the standard analyte solutions, we can construct a calibration graph of  $(10^{\Delta E/S} - 1)$  *versus* concentration (fixed-time method)<sup>24</sup>, where  $\Delta E$  is the potential variation in a selected time interval  $\Delta t$  (usually 110 s) and  $S$  is the slope of the fluoride electrode response, which is determined periodically by successive additions of micro-amounts of  $100 \mu\text{L}$  of  $1.0 \times 10^{-2}$ – $3.0 \text{ M}$  NaF standard solutions in  $25.0 \text{ mL}$  of water mixed with  $2.0 \text{ mL}$  of buffer solution.

The simultaneous determination of Al(III) and Fe(II) standard solutions with HPSAM was performed by measuring the potential changes ( $\Delta E$ ) at 80 and 110 s after initiation of the reaction for each sample solution. Then plots of HPSAM of  $(10^{\Delta E/S} - 1)$  *versus* added concentration of Al(III) were constructed for mixtures of Al(III) and Fe(II). Simultaneous determination of Al(III) and Fe(II) with PLS and PCR methods was performed by recording the potential for each solution from 20 to 150 s.

## RESULTS AND DISCUSSION

A series of experiments were conducted to establish the optimum analytical to achieve maximum sensitivity in the determination of Al(III) and Fe(II). The experimental parameters, such as PAA and fluoride concentrations, temperature and pH of solutions were optimized.

**Study of electrode characteristics:** The fast response of FISE and its Nernstian behaviour toward fluoride ions in acidic solutions indicates that this electrode might be employed effectively in the studies of reactions involving changes in the fluoride ion concentration. The characteristics of the fluoride-selective electrode in the acetate buffer were studied. In order to evaluate the operating characteristics of the FISE at  $\text{pH} < 4$ , calibration graphs were constructed for sodium fluoride in the concentration range of  $1.0 \times 10^{-2}$ – $1.0 \times 10^{-6}$  M at pHs 4.0, 3.0, 2.5 and 2.0. The slope was found to be 56.5 mV/decade and remained almost constant to 0.2 mV over 7 months of usage in this system at pH 3.0.

**Effect of fluoride concentration:** The effect of  $\text{F}^-$  concentration over the ranges of  $1.0 \times 10^{-5}$ – $1.0 \times 10^{-2}$  M fluoride ion on the linear range of calibration graph and reaction rate with Al(III) and Fe(II) was investigated. When the concentration of  $\text{F}^-$  is low, a gradual slope in the calibration graph is realized while a high concentration of  $\text{F}^-$  produces is high a steep slope in the calibration graph. The results also indicate that the concentration of  $\text{F}^-$  has a great effect on the linear range and the change potential value. So the fluoride concentration must be in excess, but by increasing the fluoride concentration, the potential change is decreased and the sensitivity is lower. If the fluoride concentration is too low, the potential may not be steady. Since, maximum differences in kinetic behaviour of Fe(III) (resulted from oxidation reaction of  $\text{Fe}^{2+}$  to  $\text{Fe}^{3+}$ ) and Al(III) were observed in concentration of  $1.0 \times 10^{-3}$  M fluoride and both species also had larger values of potential change ( $\Delta E$ ) in this concentration. Therefore, a concentration of  $1.0 \times 10^{-3}$  M fluoride was selected as the optimum concentration for further studies.

**Effect of pH:** Acidity of the solution influences both potential response of FISE and the complexation reaction rate of  $\text{F}^-$  with  $\text{Al}^{3+}$  and  $\text{Fe}^{3+}$ . The effect of pH on the reaction rate of  $\text{Fe}^{3+}$  and  $\text{Al}^{3+}$  with  $\text{F}^-$  over the pH range of 1.0 to 4.0 was examined (Fig. 4). The results show that the maximum differences in kinetic behaviour of  $\text{Fe}^{3+}$  and  $\text{Al}^{3+}$  were observed at pH 3.0. In addition, both  $\text{Fe}^{3+}$  and  $\text{Al}^{3+}$  had larger values of potential change ( $\Delta E$ ) in this pH. Above pH 3.0, the potential change decreased evidently due to the occurrence of the hydrolysis reaction competing with the complexation between fluoride and metal ions and under pH 3.0, the potential change decreased too, probably owing to the formation of hydrogen fluoride, to which the fluoride electrode is insensitive. Thus, pH of 3.0 was selected as the optimum pH for further studies.

**Effect of oxidant type and concentration:** The change of potential value ( $\Delta E$ ) for oxidation reaction of Fe(II) with certain amount of fluoride ion in different oxidant solutions such as  $\text{H}_2\text{O}_2$ , PAA,  $\text{MnO}_4^-$ ,  $\text{Cr}_2\text{O}_7^{2-}$ ,  $\text{CrO}_4^{2-}$  and Ce(IV) with different concentrations was investigated. According to obtained results, both  $\text{H}_2\text{O}_2$  and PAA were the best that showed more different kinetic behaviour for Al(III) and Fe(II), but in 0.05 M PAA solution,  $\Delta E_{\text{Fe}^{3+}}$  had larger values. Therefore, a solution of 0.05 M PAA was selected as the suitable oxidant for further studies.

**Effect of temperature:** The temperature of solution evidently affects the reaction rate of the kinetic reaction. But higher temperatures do not have a positive effect on the complexing reaction of metal ions with fluoride. Therefore, the temperature of solution was kept at  $25 \pm 0.2$  °C by thermostatic water bath in all of the measurements.

**Potential-time behaviour:** The potential-time behaviour of reactions of  $F^-$  with  $Fe^{3+}$  (resulted from oxidation of  $Fe^{2+}$  to  $Fe^{3+}$ ),  $Al^{3+}$  and mixtures of them under the optimized conditions is shown in Fig. 1. Fig. 2 shows typical reaction curves for the reaction of  $F^-$  with  $Al^{3+}$  and  $Fe^{2+}$  at different concentrations. As can be seen in Figs. 1 and 2, the reaction of  $Fe^{3+}$  is faster than  $Al^{3+}$  and was almost completed in 30 s after initial reaction but the reaction of  $Al^{3+}$  was very slow and not completed yet in this time. This difference in the reaction rates allowed us to design the HPSAM and PLS method for simultaneous determination of  $Al^{3+}$  and  $Fe^{2+}$ .

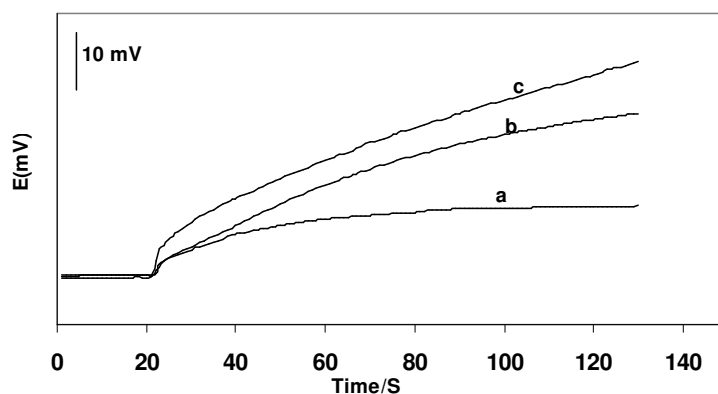
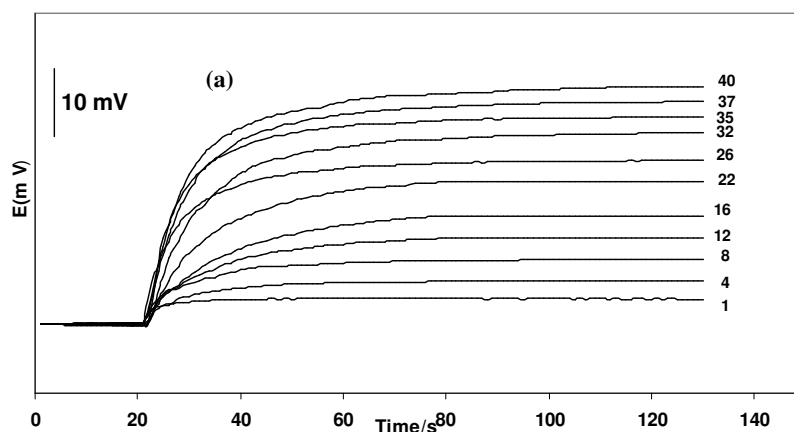


Fig. 1. Potential-time curves for the reaction of  $F^-$  with  $7.0 \mu\text{g mL}^{-1}$  of  $Fe^{2+}$  (a),  $5.0 \mu\text{g mL}^{-1}$  of  $Al^{3+}$  (b) and mixture of them (c) in the presence of PAA



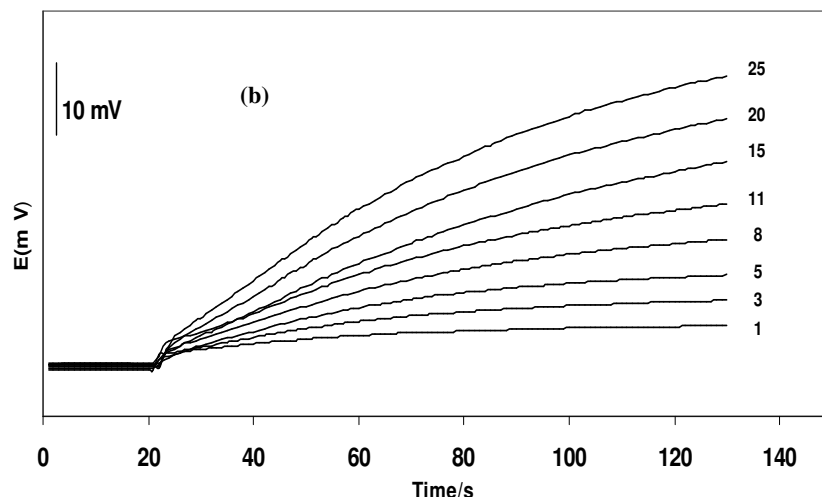


Fig. 2. Typical potential-time curves for the reaction of  $F^-$  with  $Al^{3+}$  and  $Fe^{2+}$  at different concentrations ( $\mu g mL^{-1}$ ) in the presence of PAA

Characteristics of calibration graphs for the determination of  $Al^{3+}$  and  $Fe^{3+}$ , under the optimum conditions, are given in Table-1.

TABLE-1  
CHARACTERISTIC OF CALIBRATION GRAPHS FOR THE  
DETERMINATION OF  $Fe^{2+}$  AND  $Al^{3+}$

Species	Linear range ( $\mu g mL^{-1}$ )	Slope ( $mL \mu g^{-1}$ )	Intercept	Correlation coefficient ( $n = 10$ )	Detection limit* ( $\mu g mL^{-1}$ )
$Fe^{2+}$	0.5-40.0	0.0998	0.0598	0.9996	0.15
$Al^{3+}$	1.0-25.0	0.9658	-0.3518	0.9990	0.50

\*Concentration corresponding to a net analytical signal equals to three times the standard deviation of the blank.

**Requirements for applying HPSAM:** Principles of using HPSAM for treating kinetic data upon the completion of the reaction of one component is completed while that of other component is not completed yet, is described below. In this case, the variables to be fixed were time variables  $t_1$  and  $t_2$  the product of the reaction of  $Al^{3+}$  had the same amount of R (or  $10^{\Delta E/S} - 1$ ) over the interval between these 2 times. Moreover, there is an appropriate difference between the slopes of the calibration lines in this interval.

In this special system,  $Al^{3+}$  and  $Fe^{2+}$  were considered as the analyte and interferent, respectively. Considering a binary mixture of  $Al^{3+}$  and  $Fe^{2+}$ , for example, assume that the amount of  $(10^{\Delta E/S} - 1)$  of the complexation in the reaction of  $Al^{3+}$  with  $F^-$  at time variables  $t_1$  and  $t_2$  are  $P_1$  and  $R_i$ , respectively, while those for the  $Fe^{3+} - F^-$  reaction under the same conditions are  $P$  and  $R'$ , respectively (Fig. 3). They are equal in this case. The following equations show the relation between them:

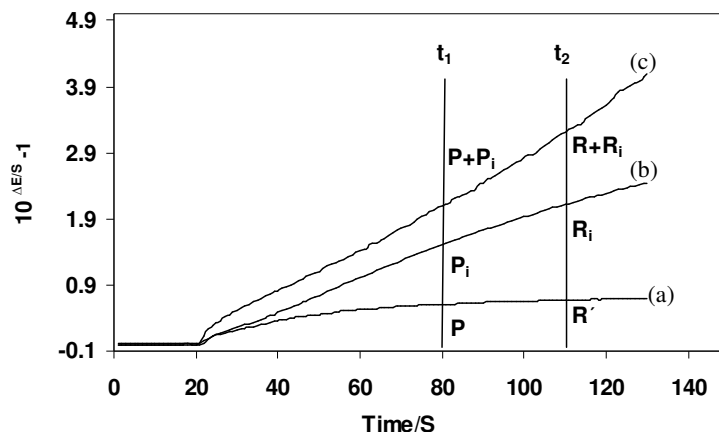


Fig. 3. Plot of potential changes ( $10^{\Delta E/S} - 1$ ) for the reaction of  $F^-$  with  $7.0 \mu g mL^{-1}$  of  $Fe^{2+}$  (a),  $5.0 \mu g mL^{-1}$  of  $Al^{3+}$  (b) and mixture of them (c) in the presence of PAA

$$\text{For Al: } R_i = P_i + m_i t_j \quad (t_1 = t_j = t_2; i = 0, 1, \dots, n) \quad (1)$$

$$\text{For Fe: } R' = P + m t_j \quad (m = 0) \quad (2)$$

where subscripts  $i$  and  $j$  denote different solutions for  $n$  additions of  $Al^{3+}$  concentration prepared to apply to HPSAM and the time comprising the  $t_1$ - $t_2$  range, respectively.

Because of the selected of  $Al^{3+}$  as analyte, it is possible to select several pairs of time where they present the same signal for  $Fe^{2+}$ . Some of the selected time pairs were 80-100, 70-85, 70-90, 90-120, 80-110. Fig. 4 shows the H-point standard addition plots for sample solution at some of the different pairs of times chosen when  $Al^{3+}$  was added. As shown previously by Campins-Falco *et al.*<sup>25</sup>, greater time increments caused higher sensitivity and steeper slopes of the 2 time axes. For this reason, the time pair of 80-110 s was employed as the most suitable times was employed.

In this case, the variables to be fixed were the times 80-110, at which the product of the reaction of  $Al^{3+}$  had the same amount of ( $10^{\Delta E/S} - 1$ ) over the range between these two times and also there is an appropriate difference between the slopes of the calibration lines.

$$\text{At 80s} \quad R_{80} = P + P_i \quad (3)$$

$$\text{At 110s} \quad R_{110} = R' + R_i \quad (4)$$

Application of HPSAM at 2 aforesaid times gives:

$$R_{80} = (10^{\Delta E(80)/S} - 1)_{80} = P_0 + P + M_{80} C_i \quad (5)$$

$$R_{110} = (10^{\Delta E(110)/S} - 1)_{110} = R_0 + R' + M_{110} C_i \quad (6)$$

where,  $\Delta E(80)$  and  $\Delta E(110)$  are the potential changes measured at 80 and 110s, respectively.  $P_0$  and  $R_0$  are the amounts of  $R$  of the  $Al^{3+}$  at sample at 80 and 110s,

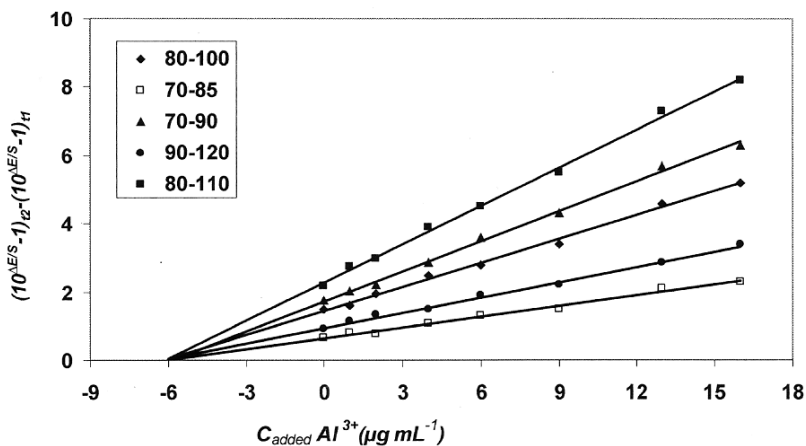


Fig. 4.  $\Delta R$  vs. added  $\text{Al}^{3+}$  concentration at different time intervals for synthetic mixtures containing  $20.0 \mu\text{g mL}^{-1}$  of  $\text{Al}^{3+}$  and  $6.0 \mu\text{g mL}^{-1}$  of  $\text{Fe}^{2+}$

respectively.  $P$  and  $R'$  are the amounts of  $R$  of the  $\text{Fe}^{3+}$  (resulted from oxidation of  $\text{Fe}^{2+}$  to  $\text{Fe}^{3+}$ ) at 80 and 110 s, respectively (Fig. 4).  $M_{80}$  and  $M_{110}$  are the slopes of the standard addition calibration lines at 80 and 110, respectively.  $C_i$  is the added  $\text{Al}^{3+}$  concentration. Two straight lines obtained intersect at the so-called H-point ( $-C_H$ ,  $R_H$ ), which at point H (Fig. 5), since  $R_{80} = R_{110}$ ,  $C_i = -C_H$ ,  $H(-C_H, R_H) \approx (-C_{\text{Al}}, R_{\text{Fe}})$  from eqns. 1 and 2 it follow that:

$$P_0 + P + M_{80}(-C_H) = R_0 + R' + M_{110}(-C_H) \quad (7)$$

$$-C_H = [(R' - P) + (R_0 - P_0)] / (M_{80} - M_{110}) \quad (8)$$

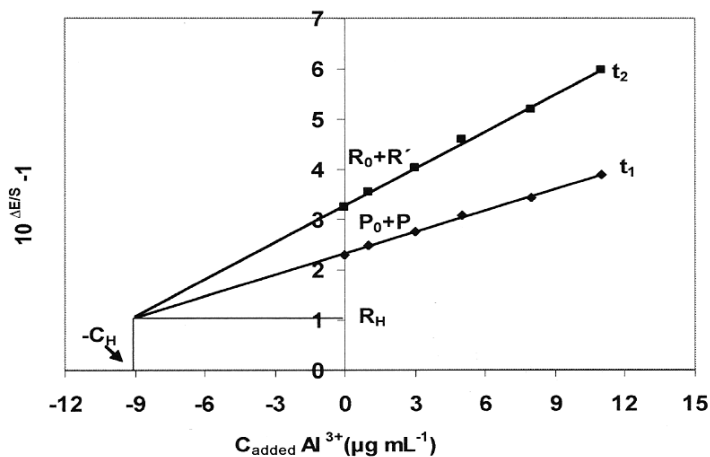


Fig. 5. Plot of HPSAM for simultaneous determination of a mixture of  $\text{Al}^{3+}$  ( $9.0 \mu\text{g mL}^{-1}$ ) and  $\text{Fe}^{2+}$  ( $10.0 \mu\text{g mL}^{-1}$ )



Because of the fast reaction between  $\text{Fe}^{3+}$  and fluoride ion, the species  $\text{Fe}^{2+}$  is assumed not to evolve over the considered range of time:

$$R' = P$$

and

$$C_H = (R_0 - P_0)/(M_{80} - M_{110}) \quad (9)$$

which is equivalent to the existing  $C_{Al}$  ( $=P_0/M_{80} = R_0/M_{110}$ ). Combining this with eqn. 5 yields  $R_H = P$ . The overall equation for the potential at the H-point is simply represented as:

$$R' = P = R_H = R_{Fe} \quad (10)$$

The intersection of the straight lines (eqns. 5 and 6) directly yields the unknown  $\text{Al}^{3+}$  concentration ( $C_{Al}$ ) and the R of  $\text{Fe}^{3+}$  (resulted from oxidation of  $\text{Fe}^{2+}$  to  $\text{Fe}^{3+}$ ) species ( $R_{Fe}$ ) corresponding to 80 and 110 in the original samples. The concentration of later species ( $C_{Fe}$ ) was calculated from this analytical signal and then calculation the concentration of  $\text{Fe}^{2+}$  from its calibration graph.

A condensation of the obtained results for various analyte concentrations is given in Table-2. As shown  $C_{Al}$  was independent of the concentration of  $\text{Fe}^{2+}$  and also the value of  $C_{Fe}$  was independent of the amount of  $\text{Al}^{3+}$  in the sample.

TABLE-2  
RESULTS OF EXPERIMENTS FOR THE ANALYSIS OF  $\text{Fe}^{2+}$  AND  $\text{Al}^{3+}$   
MIXTURES AT DIFFERENT CONCENTRATION RATIOS BY HPSAM

R-C equation	r	Spiked ( $\mu\text{g mL}^{-1}$ )		Found ( $\mu\text{g mL}^{-1}$ )	
		$\text{Fe}^{2+}$	$\text{Al}^{3+}$	$\text{Fe}^{2+}$	$\text{Al}^{3+}$
$R_{110} = 0.2483C_i + 0.8678$	0.9958	3	2	2.92(97)	2.80(104)
$R_{80} = 0.1396C_i + 0.6416$	0.9945				
$R_{110} = 0.1315C_i + 1.2068$	0.9936	4	6	3.76(94)	6.54(109)
$R_{80} = 0.0232C_i + 0.8010$	0.9923				
$R_{110} = 0.2443C_i + 0.7930$	0.9912	5	1	4.85(97)	1.04(104)
$R_{80} = 0.0849C_i + 0.6272$	0.9935				
$R_{110} = 0.2448C_i + 3.2875$	0.9946	10	9	9.50(95)	9.32(103)
$R_{80} = 0.1419C_i + 2.3277$	0.9914				
$R_{110} = 0.3956C_i + 5.1531$	0.9984	25	6	26.3(105.3)	5.82(97.0)
$R_{80} = 0.1849C_i + 3.8143$	0.9976				

**Accuracy and precision of HPSAM:** Since simultaneous determination of  $\text{Fe}^{2+}$  and  $\text{Al}^{3+}$  in different binary mixtures under the optimum conditions was made using the HPSAM. As Tables 2 and 3 show that accuracy and precision of the method is satisfactory.

**Partial least squares (PLS) and principle component regression (PCR) methods:** Multivariate calibration methods such as PLS and PCR require a suitable experimental design of the standard belonging to the calibration set in order to provide good prediction. For constructing the calibration set, factorial design was applied to 5 levels to extract a great deal of quantitative information using only a

$$\text{PRESS} = \sum_{i=1}^m (\hat{C}_i - C_i)^2 \quad (11)$$

TABLE-3  
RESULTS OF FIVE REPLICATE EXPERIMENTS FOR ANALYSIS OF  
Fe<sup>2+</sup> AND Al<sup>3+</sup> MIXTURE USING HPSAM

R-C equation	r	Spiked (µg mL <sup>-1</sup> )		Found (µg mL <sup>-1</sup> )	
		Fe <sup>2+</sup>	Al <sup>3+</sup>	Fe <sup>2+</sup>	Al <sup>3+</sup>
R <sub>110</sub> = 0.3335Ci + 1.2104	0.9998	8	1	8.16	1.007
R <sub>80</sub> = 0.1579Ci + 1.0334	0.9957				
R <sub>110</sub> = 0.3271Ci + 1.1885	0.9968	8	1	7.92	1.06
R <sub>80</sub> = 0.1961Ci + 1.0597	0.9942				
R <sub>110</sub> = 0.3118Ci + 1.178	0.9962	8	1	8.2	0.96
R <sub>80</sub> = 0.1853Ci + 1.0563	0.9950				
R <sub>110</sub> = 0.3325Ci + 1.1905	0.9935	8	1	7.94	1.02
R <sub>80</sub> = 0.1577Ci + 1.0425	0.9907				
R <sub>110</sub> = 0.3344Ci + 1.1553	0.9922	8	1	7.71	0.97
R <sub>80</sub> = 0.1579Ci + 0.9834	0.9934				
Mean				8.01	1.00
SD				0.16	0.04
RSD (%)				1.20	4.00

few experimental trials. In this research there were 33 different solutions of Fe<sup>2+</sup> and Al<sup>3+</sup> mixture. A number of 25 binary mixtures at different levels were selected as the calibration model (Table-4). The obtained model was validated with a 8 synthetic mixture set containing the considered Fe<sup>2+</sup> and Al<sup>3+</sup> concentrations in different proportions as the prediction set that were randomly selected (Table-5). The potential changes of the solutions were recorded during a time period 150 s.

TABLE-4  
CALIBRATION AND PREDICATION SETS FOR CONSTRUCTING PLS MODEL AND  
DETERMINATION OF Fe<sup>2+</sup> AND Al<sup>3+</sup> (µg mL<sup>-1</sup>)

Sample No.	Fe <sup>2+</sup>	Al <sup>3+</sup>	Sample No.	Fe <sup>2+</sup>	Al <sup>3+</sup>
1	3	3	14	12	9
2	3	6	15	12	11
3	3	8	16	12	15
4	5	2	17	12	16
5	5	4	18	14	8
6	7	2	19	14	9
7	7	3	20	14	10
8	8	1	21	17	5
9	8	2	22	17	17
10	8	4	23	25	9
11	10	9	24	25	10
12	10	10	25	25	12
13	10	14	–	–	–

To select the number of factors in the PLS algorithm a cross-validation, leaving out one sample methods was employed<sup>26</sup>. The prediction error was calculated for each species for the prediction set. This error was expressed as the prediction residual error sum of squares (PRESS):

TABLE-5  
PREDICATION SET OF CONSTRUCTING PLS AND PCR  
METHODS IN DETERMINATION OF Fe<sup>2+</sup> AND Al<sup>3+</sup>

Solution	Synthetic ( $\mu\text{g mL}^{-1}$ )		Predicted ( $\mu\text{g mL}^{-1}$ )			
	Fe <sup>2+</sup>	Al <sup>3+</sup>	PLS		PCR	
			Fe <sup>2+</sup>	Al <sup>3+</sup>	Fe <sup>2+</sup>	Al <sup>3+</sup>
1	5	3	4.81(96.2)	3.23(107.7)	4.72(94.4)	3.32(110.7)
2	12	12	12.08(100.7)	11.69(97.4)	12.10(100.8)	11.45(95.4)
3	25	11	24.03(96.1)	11.59(105.4)	23.91(95.6)	10.73(97.5)
4	3	7	3.12(104.0)	7.41(105.8)	3.19(106.3)	6.94(99.1)
5	22	14	20.68(94.0)	13.92(99.4)	20.65(93.9)	14.32(102.3)
6	5	10	4.66(93.2)	9.40(94.0)	5.35(96.6)	10.45(104.5)
7	17	9	17.21(101.2)	9.33(103.7)	17.50(102.9)	9.52(105.8)
8	10	15	10.23(102.3)	14.66(97.7)	9.85(98.5)	14.34(95.6)

$$\text{RMSEP} = \left( \sum_{i=1}^N \left( \hat{C}_i - C_i \right)^2 / n \right)^{1/2} \quad (12)$$

where  $m$  is the total number of calibration sample,  $\hat{C}_i$  represents the estimated concentration and  $C_i$  is the reference concentration for the  $i$ th sample left out of the calibration during cross validation. Fig. 6 shows a plot of PRESS against the number of factors for mixture of components. To find minimum factors, the F-statistic was also used to carry out the significant determination<sup>26</sup>. The optimal number of factors for the two components were obtained as 3.

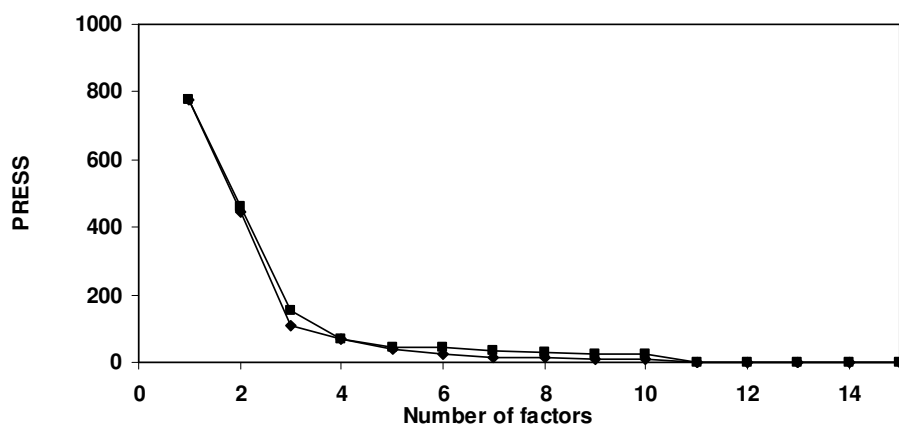


Fig. 6. Plot of PRESS against the numbers of factors for PLS (◆) and PCR (■)

For the evaluation of the predictive ability of a multivariate calibration model, the root mean square error of prediction (RMSEP) and relative standard error of prediction (RSEP) can be used<sup>27-31</sup>.

$$\text{RSEP}(\%) = \left( \frac{\sum_{i=1}^N (\hat{C}_i - C_i)^2}{\sum_{i=1}^N (C_i)^2} \right)^{1/2} \times 100 \quad (13)$$

where  $\hat{C}_i$  represents the estimated concentration,  $C_i$  and  $n$  are the actual analyte concentration and the number of samples, respectively.

$$R^2 = \frac{\sum_{i=1}^N (\hat{C}_i - C')^2}{\sum_{j=1}^N (C_j - C')^2} \quad (14)$$

where,  $C'$  represents the mean of the actual concentration in the prediction set<sup>27</sup>.

Table-6 shows values of RSEP, RMSEP and  $R^2$  for each component using PLS and PCR. It is shown that the obtained values for the statistical parameters are almost the same for both PLS and PCR methods.

TABLE-6  
STATISTICAL PARAMETERS CALCULATED FOR THE PREDICATION SET USING PLS AND PCR METHODS

Component	RSEP		RMSEP		$R^2$	
	PLS	PCR	PLS	PCR	PLS	PCR
Fe <sup>2+</sup>	3.13	4.00	0.4573	0.5839	0.9929	0.9902
Al <sup>3+</sup>	3.92	3.56	0.4215	0.3828	0.9945	0.9903

**Interference study:** The selectivity of the methods was studied by measuring mixture of 10.0  $\mu\text{g mL}^{-1}$  of both Fe<sup>2+</sup> and Al<sup>3+</sup> in the presence of some ions and investigating the effect of foreign ions (Table-7). The tolerance limit was defined as the maximum concentration of added ion causing less than 5 % relative error.

TABLE-7  
EFFECT OF INTERFERING IONS ON THE DETERMINATION OF 10.0  $\mu\text{g mL}^{-1}$  OF BOTH Al<sup>3+</sup> AND Fe<sup>2+</sup>

Species	Tolerance ratio*
Na <sup>+</sup> , Pb <sup>2+</sup> , Ni <sup>2+</sup> , Cd <sup>2+</sup> , Hg <sup>2+</sup> , Ag <sup>+</sup> , Br <sup>-</sup> , As <sup>3+</sup> , BrO <sub>3</sub> <sup>-</sup> , Cl <sup>-</sup> , Bi <sup>3+</sup>	1000**
Mg <sup>2+</sup> , SO <sub>4</sub> <sup>2-</sup> , Mn <sup>2+</sup> , I <sup>-</sup> , IO <sub>3</sub> <sup>-</sup> , K <sup>+</sup> , Zn <sup>2+</sup> , Cu <sup>2+</sup> , Co <sup>2+</sup> , C <sub>2</sub> O <sub>4</sub> <sup>2-</sup> , CH <sub>3</sub> COO <sup>-</sup>	100
PO <sub>4</sub> <sup>3-</sup> , Ca <sup>2+</sup> , HCO <sub>3</sub> <sup>-</sup>	10
Zr <sup>4+</sup> , SCN <sup>-</sup> , S <sup>2-</sup>	1.0

\*Tolerance ratio is the ratio of the interfering species to Al<sup>3+</sup> and Fe<sup>2+</sup> mixture, which causes less than 5% relative error; \*\*Largest amount tested.

**Application:** To evaluate the analytical applicability of the proposed methods (PLS, PCR and HPSAM), known amounts of Fe<sup>2+</sup> and Al<sup>3+</sup> were spiked into different

water samples. The proposed methods were applied to determine analytes simultaneously. The results (Table-8) demonstrate that the proposed methods can be employed satisfactorily for the simultaneous determination of Fe<sup>2+</sup> and Al<sup>3+</sup> in water samples.

TABLE-8  
SIMULTANEOUS KINETIC-POTENTIOMETRIC DETERMINATION OF Fe<sup>2+</sup> AND Al<sup>3+</sup> IN  
DIFFERENT WATER SAMPLES USING HPSAM, PLS AND PLS METHODS

Sample	Spiked ( $\mu\text{g mL}^{-1}$ )		Found ( $\mu\text{g mL}^{-1}$ )					
			HPSAM		PLS		PCR	
	Fe <sup>2+</sup>	Al <sup>3+</sup>	Fe <sup>2+</sup>	Al <sup>3+</sup>	Fe <sup>2+</sup>	Al <sup>3+</sup>	Fe <sup>2+</sup>	Al <sup>3+</sup>
Sprint water	5.0	3.0	5.20( $\pm 0.31$ )	3.10( $\pm 0.10$ )	4.82( $\pm 0.23$ )	3.01( $\pm 0.32$ )	4.73( $\pm 0.17$ )	3.19( $\pm 0.14$ )
	9.0	4.0	8.53( $\pm 0.17$ )	4.23( $\pm 0.22$ )	9.11( $\pm 0.45$ )	3.95( $\pm 0.28$ )	9.50( $\pm 0.15$ )	4.15( $\pm 0.51$ )
Tap water	4.0	2.0	4.02( $\pm 0.12$ )	1.90( $\pm 0.10$ )	4.12( $\pm 0.35$ )	2.07( $\pm 0.22$ )	4.2( $\pm 0.26$ )	2.11( $\pm 0.10$ )
	6.0	3.0	6.48( $\pm 0.18$ )	3.10( $\pm 0.24$ )	6.52( $\pm 0.23$ )	3.20( $\pm 0.29$ )	6.26( $\pm 0.19$ )	3.17( $\pm 0.15$ )
Mineral water	12.0	5.0	11.63( $\pm 0.38$ )	5.10( $\pm 0.17$ )	11.57( $\pm 0.11$ )	4.89( $\pm 0.37$ )	12.12( $\pm 0.25$ )	5.23( $\pm 0.44$ )
	6.0	7.0	5.78( $\pm 0.13$ )	6.82( $\pm 0.29$ )	5.06( $\pm 0.24$ )	7.15( $\pm 0.15$ )	5.32( $\pm 0.37$ )	6.71( $\pm 0.20$ )

## Conclusion

This work using HPSAM, PCR and PLS methods in the simultaneous determination of the binary mixture of Fe<sup>2+</sup> and Al<sup>3+</sup> shows the ability and excellent performance of ISEs as detectors not only for individually determination of produced or consumed ions, but also in the simultaneous kinetic-potentiometric analysis. In addition, this paper has also demonstrated that the ability and advantages of the HPSAM and chemometrics methods such as PLS, ISEs and kinetic methods produce an attractive and excellent technique for the analysis of multi-component mixtures.

## ACKNOWLEDGEMENT

The authors wish to thank for the Payame Noor University of Ardakan for the support of this work.

## REFERENCES

1. A. Safavi, H. Abdollahi and R. Mirzajani, *Spectrochim. Acta*, **63A**, 196 (2006).
2. M.G.D. Tamba, R. Falciani, T.D. Lopez and A.G. Coedo, *Analyst*, **119**, 2081 (1994).
3. K.L. Nguyen, D.M. Lewis, M. Jolly and J. Robinson, *Water Res.*, **38**, 4039 (2004).
4. F.P. Zhang, S.P. Bi, J.R. Zhang, N.S. Bian, F. Liu and Y.Q. Yang, *Analyst*, **125**, 1299 (2000).
5. A.R. Coscione, J.C. de Andrade, R.J. Poppi, C. Mello, B. van Raij and M.F. de Abreu, *Anal. Chim. Acta*, **423**, 31 (2000).
6. P.C. Nascimento, C.L. Jost, M.V. Guterres, L.D. Del' Fabro, L.M. de Carvalho and D. Bohrer, *Talanta*, **70**, 540 (2006).
7. Y. Ni, C. Huang and S. Kokot, *Anal. Chim. Acta*, **599**, 209 (2007).
8. J. Paul, *Microchim. Acta*, **54**, 1075 (1966).
9. C. Bessant and S. Saini, *J. Electroanal. Chem.*, **489**, 76 (2000).
10. Y. Ni, L. Wang and S. Kokot, *Anal. Chim. Acta*, **412**, 185 (2000).
11. A.A. Ensafi, T. Khyamian and A. Benvidi, *Can. J. Anal. Sci. Spectro.*, **49**, 271 (2004).
12. E. Shams, H. Abdollahi, M. Yekehtaz and R. Hajian, *Talanta*, **63**, 359 (2004).

13. E. Shams, H. Abdollahi and R.Hajian, *Electroanalysis*, **17**, 1589 (2005).
14. J. Mortensen, A. Legin, A. Ipatov, A. Rudnitskaya, Y. Vlasov and K. Hjuler, *Anal. Chim. Acta*, **403**, 273 (2000).
15. M. Slama, C. Zaborosch, D. Wienke and F. Spener, *Sensor Actuat. B*, **44**, 286 (1997).
16. B. Hitzmann, A. Ritzka, R. Ulber, T. Scheper and K. Schügerl, *Anal. Chim. Acta*, **348**, 135 (1997).
17. N. Garcia-Villar, J. Saurina and S. Hernández-Cassou, *Anal. Chim. Acta*, **477**, 315 (2003).
18. A.H. Aktas and S. Yasar, *Anal. Chim. Slov.*, **51**, 273 (2004).
19. M. Akhond, J. Tashkhourian and B. Hemmateenejad, *J. Anal. Chem.*, **61**, 804 (2006).
20. Ye Ying-Zhi and Y. Luo, *Lab. Robot. Automat.*, **10**, 283 (1998).
21. M.A. Karimi, M.M. Ardakani, H. Abdollahi and F. Banifatemeh, *Anal. Sci.*, **24**, 261 (2008).
22. M.A. Karimi, H. Abdollahi, H. Karami and F. Banifatemeh, *J. Chin. Chem. Soc.*, **55**, 129 (2008).
23. M.A. Karimi, M.H. Mashhadizadeh, M.M. Ardakani and N. Sahraei, *J. Food Drug Anal.*, **16**, 39 (2008).
24. E. Athanasiou-Malaki, M.A. Koupparis and T.P. Hadjiioannou, *Anal. Chem.*, **61**, 1358 (1989).
25. P. Campins-Falco, F. Bosch-Reig and F. Blasco-Gomez, *Talanta*, **47**, 193 (1998).
26. D.M. Haaland and E.V. Thomas, *Anal. Chem.*, **60**, 1193 (1988).
27. M.A. Karimi, M.A. Taher, R.B. Ardakani and S. Abdollahzadeh, *Asian J. Chem.*, **20**, 2169 (2008).
28. M. Oue and W. Wegscheider, *Anal. Chem.*, **57**, 63 (1985).
29. M.A. Karimi, M.M. Ardakani, M.R. Hormozinezhad, R. Behjatmanesh-Ardakani and H. Amiryan, *J. Serb. Chem. Soc.*, **73**, 233 (2008).
30. M.A. Karimi, M.R. Nateghi, M. Malekzadeh, F. Banifatemeh and O. Moradlou, *Asian J. Chem.*, **19**, 4533 (2007).
31. M.A. Karimi, M.M. Ardakani and H. Amiryan, *Asian J. Chem.*, **20**, 2105 (2008).